Crystal Structure of Holo Inorganic Pyrophosphatase from *Escherichia coli* at 1.9 Å Resolution. Mechanism of Hydrolysis†

Emil H. Harutyunyan,*,‡ Vaheh Yu. Oganessyan,‡,§ Natalya N. Oganessyan,‡ Svetlana M. Avaeva,|| Tatyana I. Nazarova,|| Natalya N. Vorobyeva,|| Svetlana A. Kurilova,|| Robert Huber,§ and Timothy Mather§

Shubnikov Institute of Crystallography, Russian Academy of Sciences, Leninski pr. 59, 117333 Moscow, Russian Federation, A. N. Belozersky Institute of Physico-Chemical Biology, Moscow State University, 119899, Moscow, Russian Federation, and Max-Planck-Institut für Biochemie, Abteilung Strukturforschung, Am Klopferspitz 18A, 82152, Martinsried, Germany

Received October 21, 1996⊗

ABSTRACT: Crystalline holo inorganic pyrophosphatase from *Escherichia coli* was grown in the presence of 250 mM $MgCl_2$. The crystal structure has been solved by Patterson search techniques and refined to an *R*-factor of 17.6% at 1.9 Å resolution. The upper estimate of the root-mean-square error in atomic positions is 0.26 Å. These crystals belong to space group $P3_221$ with unit cell dimensions $a = b =$ 110.27 Å and $c = 78.17$ Å. The asymmetric unit contains a trimer of subunits, *i.e.*, half of the hexameric molecule. In the central cavity of the enzyme molecule, three Mg^{2+} ions, each shared by two subunits of the hexamer, are found. In the active sites of two crystallographically independent subunits, two Mg^{2+} ions are bound. The second active site Mg^{2+} ion is missing in the third subunit. A mechanism of catalysis is proposed whereby a water molecule activated by a Mg^{2+} ion and Tyr 55 play essential roles.

Soluble inorganic pyrophosphatases (PPases)[1] hydrolyze inorganic pyrophosphate (PP_i) to two orthophosphates (P_i), thus removing this byproduct of biosynthetic reactions and controlling the level of PP_i in the cell. PPases are strongly dependent on divalent cations with the efficiency of cations as activators decreasing in the following order: $Mg^{2+} > Zn^{2+} > Co^{2+} > Mn^{2+} > Cd^{2+}$ (Welsh et al., 1983). As shown by X-ray structure analysis of *Saccharomyces cerevisiae* pyrophosphatase (Y-PPase) (Terzyan et al., 1984), a group of 15 mostly polar amino acid residues in the active site region turned out to be conserved by sequence analysis of PPases from different species (Cooperman et al., 1992). Further high-resolution crystal structure determinations of *Thermus thermophilus* (Teplyakov et al., 1994) and E-PPase (Kankare et al., 1994; Oganessyan et al., 1994) have also revealed the unique highly conserved core structure in these enzymes despite different molecular weights of monomers and oligomeric structures. The catalytic mechanism was examined in detail in PPase from *Escherichia coli* (E-PPase) (Baykov et al., 1990; Baykov & Shestakov, 1992).

These enzymes have as many as four functional metal ions in the active site. Two metal ions are bound to PPase as essential cofactors (metal activators), whereas the third and fourth metal ions are liganded to PP_i/P_i forming substrate/product (substrate metals) (Baykov et al., 1990; Baykov & Shestakov, 1992). The close proximity of all metal ions to one another is revealed by the structure determination of the Mn^{2+},Pi·Y-PPase complex (Harutyunyan et al., 1996a). These metal ions are assumed to play a specific role in many steps of the catalytic reaction: substrate activation, the acceptance of leaving groups, and the activation of the water molecule involved in the hydrolysis of the PP_i ether bond being the most important among them. In spite of intensive studies of the PPase catalytic mechanism, the precise role of the four metal ions has remained unclear. At present and in contrast to Y-PPase, only the location of the first metal ion site with the highest affinity for the enzyme is established in the active site of E-PPase, based on X-ray analysis. In the Mn^{2+}·E-PPase structure (Harutyunyan et al., 1996b), this manganese ion is coordinated by Asp65, Asp70, and Asp102, as is one of four Mn^{2+} ions in the Mn^{2+},Pi·Y-PPase complex (Harutyunyan et al., 1996a). In the structure of the Mg^{2+} complex of E-PPase determined later (Kankare et al., 1996a), similar coordination of the active site metal ion is described.

A description of the three-dimensional structure of E-PPase complexed with two Mg^{2+} ions in the active site (holo enzyme) is an important step in understanding features of the catalytic mechanism. We succeeded in growing crystals of holo E-PPase containing both metal activators only at a very high concentration of Mg^{2+} (250 mM). In this paper, we describe the preparation of crystals and the crystal structure of E-PPase complexed with two magnesium ions in the active site. The catalytic mechanism is also discussed.

MATERIALS AND METHODS

Crystallization. The cloning, expression, purification, and crystallization studies were described previously (Oganessyan

† This work was supported by Volkswagen Stiftung and Russian Foundation for Fundamental Studies (RFFS) Grant 94-04-12727-a.

* Author to whom correspondence should be addressed. Fax: (095) 135 10 11. E-mail: emil@protein.crystal.msk.ru.

‡ Shubnikov Institute of Crystallography, Russian Academy of Sciences.

§ Max-Planck-Institut für Biochemie.

|| A. N. Belozersky Institute of Physico-Chemical Biology, Moscow State University.

⊗ Abstract published in *Advance ACS Abstracts,* January 15, 1997.

[1] Abbreviations: PPase, soluble inorganic pyrophosphatase; PP_i, inorganic pyrophosphate; P_i, orthophosphate; P_iA, attacked group of PP_i; P_iL, first living group of PP_i after hydrolysis; E-PPase, PPase from *Escherichia coli*; Mg1 and Mg2, high- and low-affinity binding Mg^{2+} ions in the active site of E-PPase; W_a, activated water molecule; Y-PPase, PPase from *Saccharomyces cerevisiae*; Mn^{2+},Pi·Y-PPase, Y-PPase complexed with four Mn^{2+} ions and two orthophosphates; Mn·E-PPase, E-PPase complexed with one Mn^{2+} ion; 1.5Mg·E-PPase, E-PPase complexed with one Mg^{2+} ion in the active site and one Mg^{2+} ion shared with the other subunit.

S0006-2960(96)02637-2 CCC: $14.00

Table 1: Data and Refinement Statistics

data set statistics		refinement statistics	
maximal resolution (Å)	1.9	root-mean-square deviations	
reflections measured	360600	bond distances (Å)	
unique reflections	41190	1−2 neighbors	0.014 (0.020)[b]
completeness (%)	99.6 (99.9)[a]	1−3 neighbors	0.031 (0.040)
completeness $>3\sigma$ (%)	87.0 (80.0)	1−4 neighbors	0.034 (0.050)
R_{sym} (%)	7.7 (24.1)	peptide planarity (Å)	0.008 (0.010)
refinement statistics		chiral volumes (Å^3)	0.142 (0.150)
resolution range (Å)	12.0−1.9	single torsion contacts (Å)	0.173 (0.300)
R/R_{free} (%)	17.6/23.2	multiple torsion contacts (Å)	0.255 (0.300)
protein atoms	4137	torsion angles (degrees)	
Mg^{2+}	7	planar	7.9 (7.0)
water molecules	250	staggered	19.4 (15.0)
average *B*-factors (Å^2)		orthonormal	22.5 (20.0)
protein atoms	34.3	temperature factors (Å^2)	
Mg^{2+}	32.5	1−2 neighbors (main chain)	1.927 (4.000)
water molecules	40.7	1−2 neighbors (side chain)	5.166 (6.000)

[a] The appropriate values in the resolution shell 1.9−1.95 Å are given. [b] The appropriate target values are given.

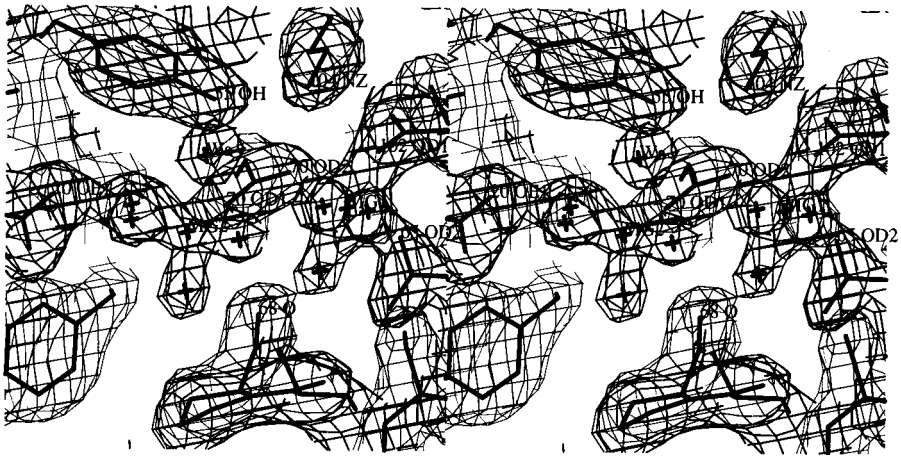

FIGURE 1: Stereoview of the final ($2F_0 - F_c$) electron density map in the region of the active site superimposed with the atomic model [prepared with "O" (Jones et al., 1991)]. Positions of Mg^{2+} and water molecules are crossed.

et al., 1994). The protein complexed with Mg^{2+} was crystallized using the crystallization conditions of the apo enzyme in hanging drops (20 μL) of 100 mM Tris-HCl buffer, pH 7.5, 25% NH_4Cl (REACHIM, Russia), and 200 μM protein, with $MgCl_2$ (MERCK) added to 250 mM, against a solution of 100 mM Tris-HCl buffer, pH 7.5, 58% NH_4Cl, and 250 mM $MgCl_2$. Within 2 weeks, rhombohedral crystals of size 0.6 × 0.6 × 0.8 mm appeared. The crystals belong to space group $P3_221$ with unit cell constants $a = b = 110.3$ Å and $c = 78.2$ Å. The asymmetric unit contains three subunits.

X-ray Data Collection. X-ray diffraction data were measured on a MAR image plate system (MAR Research, Hamburg), mounted on a Rigaku Denki rotating anode X-ray generator ($\lambda = 1.5418$ Å, operated at 5.4 kW). A total of 155 images with an oscillation range of 1° were recorded with 1 crystal and processed with the Mosflm program package (Leslie, 1994) and CCP4 suite (CCP4, 1994) (Table 1). When the data were processed with space group $P3_2$, the R_{merge} was 8.9% versus 7.7% for $P3_221$.

Refinement. The atomic model of E-PPase (form 1) refined at 2.2 Å to an *R*-factor of 16.5% (Harutyunyan et al., 1996b) was used for rotational and translational searches with AMoRe (Navaza, 1994) using 10−4 Å data. Three solutions with the highest peaks for both rotation and translation were related by a 3-fold axis parallel to *z* with $x = {}^2/_3$ and $y = 0$. Combining this 3-fold axis with the $P3_221$ space group results in the space group *R32*. The arrangement of hexameric molecules in the unit cells of both holo and apo structures thus turned out to be similar. The correlation and *R*-factor were 82% and 22% respectively.

The refinement was carried out using the CCP4 suite (CCP4, 1994) and REFMAC (Murshudov et al., 1996) with all X-ray data within resolution shells 12.0−1.9 Å, except for 7% of reflections taken out of the refinement to calculate the free *R*-factor. From the start, atomic coordinates and individual *B*-factors were refined with both $P3_2$ and $P3_221$ space groups with six and three subunits in the asymmetric unit, respectively. The overall structure turned out to be essentially the same in each case. Therefore, further refinement was carried out with $P3_221$ using alternating rounds of manual building with the program "O" (Jones et al., 1994) and positional refinement. When the *R*-factor dropped to 22%, solvent molecules were gradually included into the model if suitable peaks with height greater than 3σ in the ($F_o - F_c$) electron density map were in the distance of 2.4−4.0 Å from protein atoms.

Several peaks on the difference Fourier map turned out to be surrounded by six octahedrally arranged neighbors, either protein atoms or water molecules, at rather short distances (~2 Å). These peaks were assigned to Mg^{2+}. The second Mg^{2+} ion in the active sites of both A and B subunits, however, had higher *B*-factors than surrounding ligands. With the occupancies at 0.7 for both, the *B*-factors of these ions became comparable to those of the ligands.

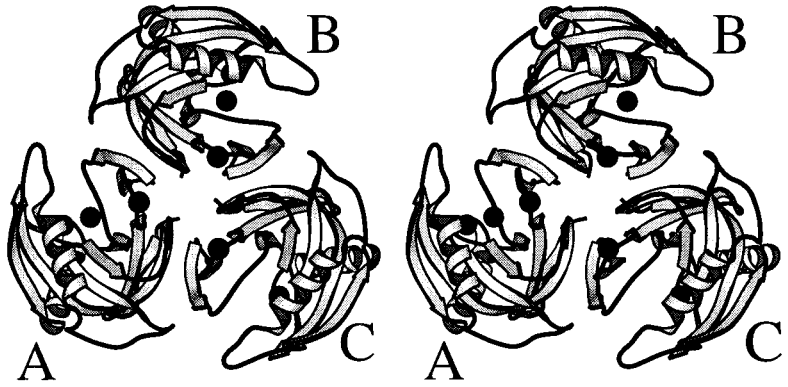

FIGURE 2: Stereo drawing of the polypeptide chain course in the trimer (subunits A, B, and C are marked). Mg^{2+} ions are shown as black spheres.

Refinement statistics for the final atomic model are given in Table 1. The electron density map in the region covering two Mg^{2+} binding sites both with full and low occupancies is shown in Figure 1. The average *B*-factor (34.3 Å^2) of the model is in agreement with that derived from the Wilson plot (34.8 Å^2).

RESULTS

Quality of the Model. The characteristics of the final atomic model are given in Table 1. All 175 amino acid residues in each of the 3 subunits in the asymmetric unit are visible in the final electron density map. Each subunit contains 1379 protein atoms and 2.5 Mg^{2+} ions except the C subunit, which contains 1.5 Mg^{2+}; 250 solvent molecules were interpreted as water molecules. The difference electron density map calculated with final atomic model phases does not contain significant peaks to suggest further refinement of the model. A Ramachandran plot calculated using PROCHECK (Morris et al., 1992) revealed no residues with main chain dihedral angles in disallowed regions; 91.4% of the amino acid residues are in the most favorable region. Other residues are in additionally allowed regions.

The overall estimate of coordinate error from the σ_A plot (Read, 1986) is 0.26 Å; *i.e.*, interatomic distances are detected with a root-mean-square deviation of 0.39 Å. Three crystallographically independent subunits of the hexamer were refined without noncrystallographic symmetry restraints. Two of them (A and B, see below) contain an equal number of magnesium ions. Root-mean-square devations between the atomic positions in these subunits are presumed to correspond to the error in evaluation of interatomic distances. Superimposition of these two subunits results in root-mean-square deviations of 0.34 Å for CA atoms, 0.34 Å for main chain atoms, and 0.68 Å for side chain atoms. The largest deviations for side chain atoms are mostly due to different positions of the side chains protruding into solvent and modeled differently in the two subunits. Among the active site residues, the deviations of the terminal atoms of Glu31, Asp42, and Asp67 (nonliganded by magnesium ions) are more than 1 Å. The positions of OE1 and OE2 of Glu31 in these two subunits deviate by 1.6 and 2.8 Å, OD1 and OD2 of Asp42 by 1.3 and 0.9 Å, and OD1 and OD2 of Asp67 by 1.3 and 0.9 Å. These residues are located at the entrance of the active site. The active site metal ions (Mg1 and Mg2) superimpose with deviations of 0.14 and 0.37 Å, respectively; deviations of their protein ligands and active site water molecules are less than 0.2 and 0.4 Å, respectively.

Root-mean-square deviations are highly correlated with temperature factors. To estimate the root-mean-square deviation for well-determined atoms, only those with temperature factors less than 55 Å^2 were superimposed. Divided by $\sqrt{2}$, these values are 0.24 Å for main chain and 0.32 Å for side chain atoms, which are in good agreement with the overall coordinate error estimate of 0.26 Å derived from the σ_A plot.

The noncrystallographic 3-fold symmetry was not imposed during refinement. No significant deviations from molecular $D_3 = 32$ were detected in terms of positions of Mg^{2+} ions and their ligands. The only discrepancies correspond to an absence of the second active site Mg^{2+} and water molecules bound to this ion in the third (C) subunit. Atomic coordinates for all three subunits are deposited in the Protein Data Bank with Identification Code xxxx.

Overall Structure of Holo E-PPase. The homohexameric apo form of E-PPase was previously crystallized in two crystalline forms depending on the precipitant used. Crystal structures, first with one subunit (form I; Harutyunyan et al., 1996b) and then a second form with two subunits in the asymmetric unit (form II; Kankare et al., 1996a), were determined at 2.2 Å resolution and described.

Crystals of holo E-PPase were grown in the same conditions as form I (Oganessyan et al., 1994) in 0.25 M $MgCl_2$. In the presence of this high concentration of magnesium ions, the enzyme crystallized with unit cell dimensions similar to those of form I. However, the space group was different, $P3_221$ instead of *R32*; *i.e.*, the asymmetric unit in the present crystals is 3 times larger and contains three subunits instead of one. Loss of the 3-fold crystallographic axis and crystallographic equivalency of three subunits in the trimer probably is caused by a subtle rearrangement of amino acid side chains in interhexameric contacts. The trimers of the enzyme molecule consisting of three crystallographically nonrelated subunits are related by a crystallographic dyad. These subunits are named A, B, and C (Figure 2).

The packing of enzyme molecules is essentially the same both in apo and holo crystals. As in apo enzyme crystals, interhexameric contacts are formed by segments 146−147 and 159−170 of A−B and C−D type pairs. However, the orientation of side chains in these regions varies slightly for different pairs of contacting subunits.

Binding of magnesium ions induces slight changes in the overall structure of the apo enzyme subunit. Root-mean-square deviations when main chain atoms of apo enzyme

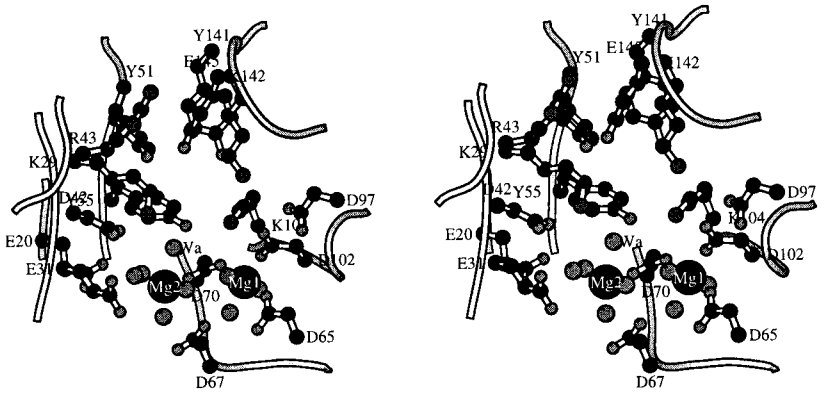

FIGURE 3: Stereoview of the active site. Terminal atoms of side chains and water molecules are gray; carbon atoms are black. Mg^{2+} ions are presented by large black spheres and marked.

were superimposed on those of each three subunits of the holo enzyme are 0.37 Å, 0.36 Å, and 0.36 Å for the A, B, and C subunits, respectively. The largest deviations are observed for polypeptide chain segments 24−30 (less than 0.5 Å), 34−38 (less than 0.5 Å), 65−66 (about 0.5 Å), 98−103 (about 1 Å at Glu98, Ala99, and Gly100; less than 0.5 Å for the rest atoms), 146−151 (0.6−1.2 Å), and 173−175 (about 1 Å). Most of these parts of the polypeptide chain were not well resolved in the apo enzyme structure (resolution 2.2 Å) and are characterized by higher temperature factors. Some parts of the polypeptide chain carrying ligands of Mg^{2+} are better stabilized in the present structure. These data show that the description of the three-dimensional structure of E-PPase determined for its apo form also applies for its holo form.

Between each pair of subunits related by a molecular dyad near the central cavity of the hexamer, a single Mg^{2+} is detected. This ion is octahedrally coordinated by six water molecules H-bonded to OD1 Asn24, OD1 Asp26, and O Asn24 from each of two subunits related by a molecular 2-fold axis [according to the "O" program (Jones et al., 1991), we specify H-bonds if donor−acceptor distances are less than 3.25 Å with angular cutoff 90]. Thus, no protein atoms are directly involved in the binding of this Mg^{2+}. The Mg−O distances are in the range of 2.1−2.2 Å.

The Active Site. From the superimposition of the enzyme structures of the apo form and the two crystallographically independent subunits of the holo form (A and C), we concluded that no essential changes occur in the positions of the active site side chains except those which are situated at the entrance. In the active sites of the A and B subunits, two Mg^{2+} with occupancies of 1.0 and 0.7 which bind in the absence of P_i or PP_i are believed to be the two metal activators. Thus, the structure of these subunits is believed to correspond to that of the holo enzyme. In the C subunit, the occupancy of the second Mg^{2+} binding site is less than 0.2. This subunit can be considered as the apo enzyme complexed only with the Mg^{2+} of highest affinity. The further descriptions are of the A subunit.

The active site is presented in Figure 3. Mg1 has octahedral coordination formed by the OD atoms from three monodentate aspartate side chains: OD2 of Asp65, OD2 of Asp70, OD1 of Asp102, and three water molecules. The octahedral coordination of Mg2 is slightly distorted. In addition to OD1 of Asp70, five water molecules are detected in the first coordination sphere of this Mg^{2+}. Thus, the side chain of Asp70 bridges two Mg^{2+} which are nearly in the plane of the carboxylate group. There is no single water

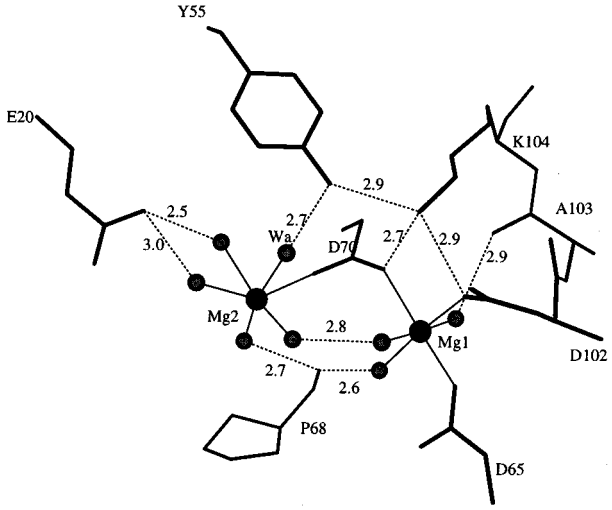

FIGURE 4: Description of coordination of Mg^{2+} (black spheres) with ligands is presented by solid lines. Side chains H-bonded (dotted lines) to Mg^{2+} ligands are included. Water molecules are shown as gray spheres.

molecule shared by two Mg^{2+}. All interatomic distances between both Mg^{2+} and their ligands lie in the range 2.0−2.2 Å, except Mg2−W_a at 2.6 Å (2.3 Å in the B subunit). This water molecule (W_a) makes a hydrogen bond to OH of Tyr55 at 2.7 Å and is believed to be the attacking group during PP_i hydrolysis (see below). In the apo form, OH of Tyr55 is H-bonded to the water molecule nearest to the W_a location, at a distance of 3.5 Å. Two water molecules liganded by the different Mg^{2+} are in H-bonding distance to each other and do not have any protein ligands. All other water molecules, liganded by Mg^{2+}, are H-bonded by enzyme (Figure 4).

The binding site of Mg1 corresponds to the single metal ion binding site found in the active center both in the Mn·E-PPase (Harutyunyan et al., 1996b) and in 1.5Mg·E-PPase (Kankare et al., 1996b) complexes and is shown to be the metal activator binding site with highest affinity (Baykov et al., 1996). Both Mg1 and Mg2 binding sites found in the present structure correspond to those of two Mn^{2+} in the structure of yeast PPase which were assumed to be two metal activators (Harutyunyan et al., 1996a).

In Figure 5, the arrangement of water molecules found in the active site both of the apo and of the holo forms is presented. Binding of metal ions leads to changes both in the amount of bound solvent molecules and in their location in the active site. Accompanied by displacements of protein side chains, this changes the hydrogen bond network. Three

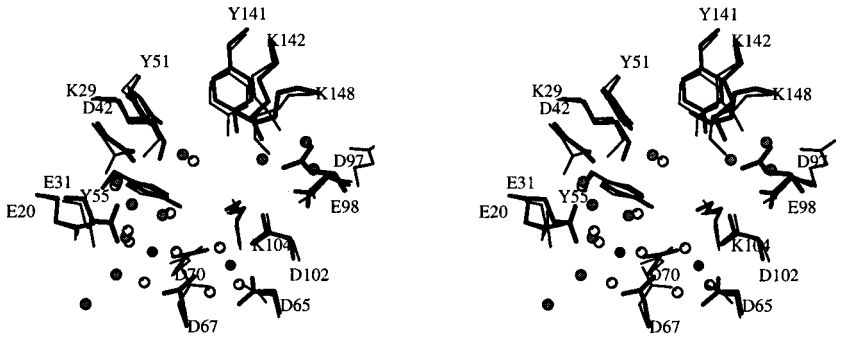

FIGURE 5: Arrangement of the water molecules (white spheres in holo enzyme, gray spheres in apo enzyme) and Mg^{2+} (black spheres) in the active sites of both apo (thin lines) and holo (thick lines) enzymes when superimposed with CA atoms.

water molecules bound to Mg1 are not found in the structure of the apo enzyme form I (Harutyunyan et al., 1996b) while they were detected in form II (Kankare et al., 1996b). In contrast, at least two water molecules from the five liganded to Mg2 are detected also in the apo enzyme structure with deviations in their positions of 0.5 and 1.0 Å (W_a). In the structure of Mn·E-PPase containing a single Mn^{2+} (in the position of Mg1) (Harutyunyan et al., 1996b), three such water molecules corresponding to those which would bind to the second metal activator are also determined.

Five water molecules from 10 found in the apo form are not present in the holo form. They mostly are replaced by protein side chains involved in the binding of substrate or substrate metals as seen also in the structure of Mn,Pi·Y-PPase complex (Harutyunyan et al., 1996a). Thus, the side chain of Glu98 situated at the entrance enters the active site region to replace two water molecules and to orient through H-bonds both Lys142 and Lys148. The side chain of Glu31 also turns into the active site and supplants a water molecule. Besides two water molecules coordinated by Mg2, three others are also conserved in both enzyme forms. They are located deeper in the active site and H-bonded to Lys29 NZ, Tyr51 OH, and Tyr141 OH.

DISCUSSION

Binding of Metal Ions. Our long-term crystallization experiments conducted with preincubated enzyme at increasing (up to 100 mM) concentrations of $MgCl_2$, to prepare E-PPase complexed with two Mg^{2+} in the active site, were not successful. The crystalline complex we obtained consistently contained only one Mg^{2+} in the active site with an additional ion bound in the intersubunit region (unpublished data). Soaking of the crystals at concentrations of $MgCl_2$ up to 140 mM also results in formation of enzyme complex containing only a single Mg^{2+} in the active site region and one additional Mg^{2+} in the intersubunit region (Kankare et al., 1996b). On the other hand, the Mn^{2+}·E-PPase prepared with only 0.1 mM $MnCl_2$ contains a single metal ion in the active site with highest affinity. These results show that the affinity of the enzyme for the second metal activator is much less than that for a metal ion found in the intersubunit region.

However, there is sufficient evidence to believe that the enzyme molecule requires two bound metal ions in the active site to be activated. Stoichiometric results from kinetic studies indicating this (Baykov et al., 1990; Baykov & Shestakov, 1992) are supported by X-ray structure analysis of Y-PPase complexed with reaction products (Harutyunyan et al., 1996a).

Mechanism of Catalysis. Hydrolysis of PP_i catalyzed by PPases proceeds according to the following scheme (*e.g.*, Cooperman et al., 1992):

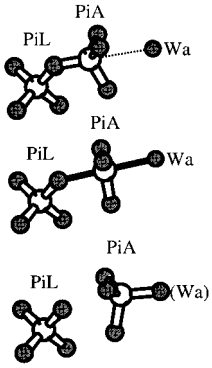

FIGURE 6: Scheme of formation of the transition state.

$$Mg_2\cdot E \rightleftarrows Mg_2\cdot E\cdot Mg_2PP_i \underset{2}{\overset{H_2O}{\rightleftharpoons}}$$
$$Mg_2\cdot E\cdot 2(MgP_i) \underset{3}{\rightleftarrows} Mg_2\cdot E\cdot MgP_i \underset{4}{\rightleftarrows} Mg_2\cdot E$$

No formation of phosphorylated enzyme appears to occur during the reaction (Gonzalez et al., 1984). Stage 2 includes formation of the transition state with the attacked P_i (Pi_A) and attacking activated water molecule W_a (Figure 6). Formation of the transition state, with trigonal bipyramidal coordination of the P_iA phosphorus atom carrying the ether oxygen and W_a in the apical positions, seems to be most likely, as all three non-ether oxygen atoms are chemically equivalent and the P−O bond with the ether oxygen is significantly weakened. It may be assumed as described earlier (Harutyunyan et al., 1996a) that in the transition state, the phosphorus atom of P_iA moves toward the approaching attacking water molecule (W_a) rather than that the three P_iA oxygen atoms are simply inverted. This process could be facilitated if the P−O bonds of P_iA are weakened due to interactions with metal ions and positively charged protein groups. The remoteness of the W_a from P_iL (leaving P_i) should be taken into account when its binding site is considered.

Structural data on yeast PPase complexed with its reaction products (4 Mn^{2+} and 2 P_i) are in agreement with this hypothesis (Harutyunyan et al., 1996a). In the structure, P_iL and P_iA were attached to two and four Mn^{2+} ions, rspectively. Consistent with this observation, their binding sites were attributed to those of the leaving and attacked P_i groups of the PP_i hydrolysis, respectively. The region of the active site adjoining one of the Mn^{2+} (believed to be the second metal activator), Tyr93 (Tyr55 in the E-PPase), and Lys154 (Lys104) was suggested to be the location of the attacking water molecule (Harutyunyan et al., 1996a). The structure

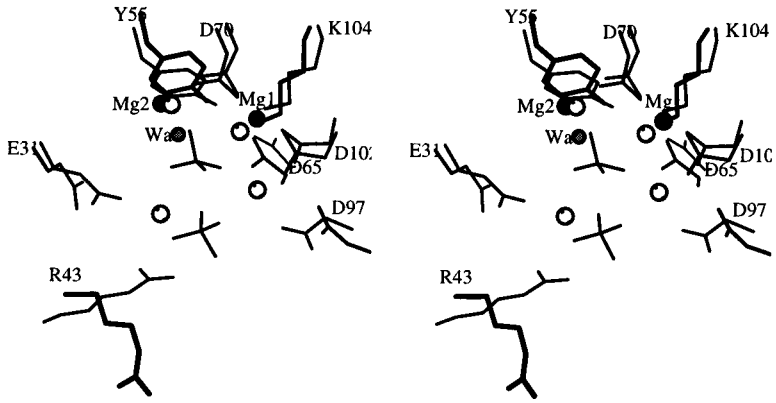

FIGURE 7: Stereoview of E-PPase (thick lines) and Y-PPase (thin lines) with active sites superimposed (see text). Mg^{2+} (black), Mn^{2+} (white), the attacking water molecule (W_a), and P_i groups in Y-PPase are shown.

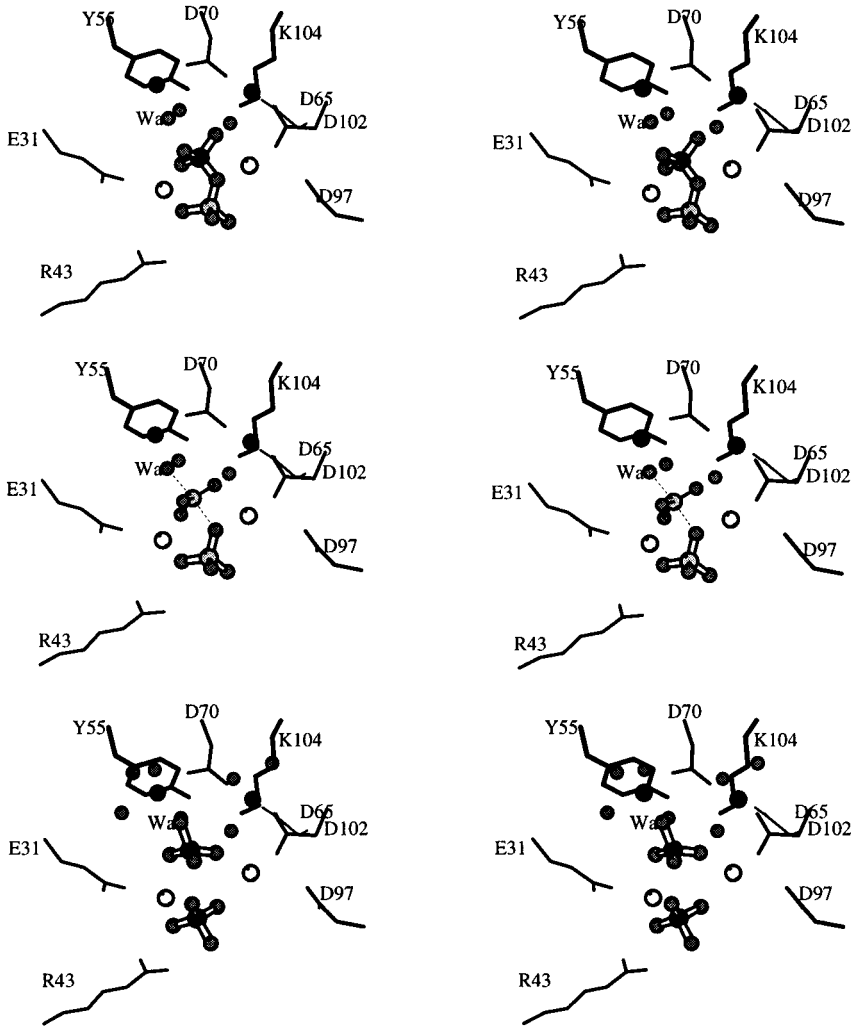

FIGURE 8: Stereo schematic presentation of the active site at the consecutive steps of PP_i hydrolysis: Michaelis complex with attacking water molecule W_a (a); transition state (b); and complex with products (c). Trigonal-bipyramidal coordination of P at the transition state is presented by thin and dashed lines in contrast to P_i groups (ball and stick). Activating metals are black, and substrate metals are white.

of the holo enzyme is most important to examine these assumptions.

The present structure of holo E-PPase was compared with the structure of yeast PPase, complexed with the reaction products to determine the possible location of the substrate and water molecule to be activated, as well as those groups which could be responsible for the activation of the water molecule. All atoms of the residues participating in the binding of metal ions and P_i groups were used for superimposition (in parentheses the numbers of residues in yeast PPase are given): Lys29 (56), Glu31 (58), Asp42 (77), Tyr51 (89), Tyr55 (93), Asp65 (115), Asp67 (117), Asp70 (120), Asp97 (147), Glu98 (148), Asp102 (152), Lys104 (154), Tyr141 (192), Lys142 (193). The root-mean-square deviation was 1.39 Å, and the maximal deviation for OD1 Asp42 was 2.36 Å. Deviations in positions of the two metal activators were 1.2 and 0.7 Å, respectively, which encouraged further consideration.

The two superimposed structures are shown in Figure 7. Mg2 carries a weakly bound water molecule, W_a, at a distance of 2.6 and 2.3 Å in the A and B subunits, respectively. Being H-bonded to the OH of Tyr55, this water

molecule is the nearest among the water molecules coordinated to Mg^{2+} to the P_iA. The deviation between position of W_a and that of O1 P_iA in the Y-PPase complex was found to be about 0.7 Å. Thus, the identification of the attacking water molecule binding site is supported by the Y-PPase complex structure.

The W_a makes its only H-bond to OH Tyr55, which may be suggested as the acceptor of a proton when W_a is activated. Independent support of this assumption is the decrease in p*K* of Tyr55 when the second metal activator is bound to the enzyme (Avaeva et al., 1995).

The subsequent step was modeling of two P_i moieties into the active site region. One P_i was put with distances of 2.7 Å between its three oxygen atoms and W_a. The second P_i was placed so that its phosphorus and two oxygen atoms are in the plane of the Arg43 guanidinium group [taken from the structure of a form containing a sulfate H-bonded to Arg43 (V.Yu.O. et al., unpublished data)] with two O−NH distances at 2.7 Å. Such placement brings two oxygen atoms (one from each P_i) to nearly the same position (0.3 Å deviation), both indicating the position of the ether oxygen when two P_i are combined into PP_i (Figure 8a). All metal ions are at appropriate distances from P_i oxygen atoms except Mg1 in the present structure (more than 3 Å).

A generalized three-dimensional scheme of the transition state, deduced from the modeled structure of the Michaelis complex, is given in Figure 8b. In the proposed scheme, the positions of the substrate metal ions are taken from the structure of Y-PPase complex. One "substrate" metal ion bridges both P_i via their non-ether oxygen atoms. The second one binds a non-ether oxygen atom of P_iA and the ether oxygen atom. Four metal ions ligate P_iA, but only two substrate ions bind P_iL. According to the catalytic scheme, P_i groups leave the active site complexed with metal ions. One can assume that the P_iL and P_iA complexed with the fourth and third metal ion, respectively, leave the active site in this succession (Figure 8c).

Conclusions. Only a general scheme of catalytic reaction is discussed. No essential displacements of the reaction participants, *i.e.*, protein side chains, metal ions, substrate, and water molecules, are taken into account, as structures of PPases from different species are considered. For confident conclusions about displacements, most of them being small, high-resolution structural data on apo and holo forms, complexes with substrate analogs, and reaction products are still of great interest. Crystallization of these complexes has met with difficulties despite numerous studies performed by crystallographic groups in Turku and Moscow. The reasons for failures may result from the presence of high concentrations of monovalent cations in mother liquids. On the other hand, purification of the enzymes could lead to removal of any metal cations from the endogenous enzyme, which may cause slowly reversible conformational changes in the molecular structure which hinder binding of cations with lower affinity for the enzyme.

In the active site of PPases, an extensive hydrogen-bonding network is formed by water molecules and side chains of aspartates, glutamates, lysines, and tyrosines participating directly or via water molecules in the binding of metal ions and/or substrate. Any mutation of these residues causes a loss of enzyme activity, as metal ions and substrate cannot be bound at all, or are bound in an improper mode. Tyr55 and probably Lys104 might be an exception as they are not involved in the binding of metals. In accordance with the present results, they are presumed to participate in the activation of the attacking water molecule. This assumption would be supported if Y55F and probably K104A mutants bind metal cofactors and PP_i. Then loss of activity of these mutant forms would suggest an absence of the group which activates the substrate. Crystallization studies of these mutants are now in progress.

Crystallization and structure determination have been carried out during the visit of V.Yu.O. to the Max-Planck Institut für Biochemie in Martinsried.

ACKNOWLEDGMENT

We thank Dr. F. J. Medrano and Dr. F. X. Gomis-Rüth for their helpful assistance. V.Yu.O. and E.H.H. thank Volkswagen Stiftung for supporting their visits to the MPI für Biochemie.

REFERENCES

Avaeva, S. M., Rodina, E. V., Kurilova, S. A., Nazarova, T. I., Vorobyeva, N. N., Harutyunyan, E. H., & Oganessyan, V. Yu. (1995) *FEBS Lett. 377*, 44−46.

Baykov, A. A., & Shestakov, A. S. (1992) *Eur. J. Biochem. 206*, 463−470.

Baykov, A. A., Shestakov, A. S., Kasho, V. N., Vener, A. V., & Ivanov, A. H. (1990) *Eur. J. Biochem. 194*, 879−887.

Baykov, A. A., Hyytiä, T., Volk, S. E., Kasho, V. N., Vener, A. V., Goldman, A., Lahti, R., & Cooperman, B. S. (1996) *Biochemistry 35*, 4655−4661.

Collaborative Computational Project, Number 4 (1994) *The CCP4 Suite: Programs for Protein Crystallography*, *Acta Crystallogr. D50*, 760−763.

Cooperman, B. S., Baykov, A. A., & Lahti, R. (1992) *Trends Biochem. Sci. 17*, 262−266.

Gonzalez, M. A., Webb, M. R., Welsh, K. M., & Cooperman, B. S. (1984) *Biochemistry 23*, 797−801.

Harutyunyan, E. H., Kuranova, I. P., Vainshtein, B. K., Höhne, W. E., Lamzin, V. S., Dauter, Z., Teplyakov, A. V., & Wilson, K. S. (1996a) *Eur. J. Biochem. 239*, 220−228.

Harutyunyan (Arutyunyan), E. H., Oganessyan, V. Yu., Oganessyan, N. N., Terzyan, S. S., Popov, A. N., Rubinskiy, S. V., Vainshtein, B. K., Nazarova, T. I., Kurilova, S. A., Vorobyeva, N. N., & Avaeva, S. M. (1996b) *Kristallografia 41*, 84−96.

Jones, A. T., Zou, J. Y., Cowan, S. W., & Kjeldgaard, M. (1991) *Acta Crystallogr. A47*, 110−119.

Kankare, J., Salminen, T., Lahti, R., Cooperman, B. S., Baykov, A. A., & Goldman, A. (1996a) *Acta Crystallogr. D52*, 551−563.

Kankare, J., Salminen, T., Lahti, R., Cooperman, B. S., Baykov, A. A., & Goldman, A. (1996b) *Biochemistry 35*, 4670−4677.

Leslie, A. G. W. (1991) in *Crystallographic computing* (Moras, D., Podjarni, A. D., & Thierry, J. C., Eds.) pp 50−61, University Press, Oxford.

Morris, A. L., MacArthur, M. W., Hutchinson, E. G., & Thornton, J. M. (1992) *Proteins: Struct., Funct., Genet. 12*, 345−364.

Murshudov, G., Vagin, A., & Dodson, E. (1996) in *The Refinement of Protein Structures*, Proceedings of Daresbury Study Weekend.

Navaza, J. (1994) *Acta Crystallogr. A50*, 157−163.

Oganessyan, V. Yu., Kurilova, S. A., Vorobyeva, N. N., Nazarova, T. I., Popov, A. N., Lebedev, A. A., Avaeva, S. M., & Harutyunyan, E. H. (1994) *FEBS Lett. 348*, 301−304.

Read, R. J. (1986) *Acta Crystallogr. A42*, 140−149.

Terzyan, S. S., Voronova, A. A., Smirnova, E. A., Kuranova, I. P., Harutyunyan, E. H. (Arutyunyan, E. G.), Vainshtein, B. K., Höhne, W., & Hansen, G. (1984) *Bioorg. Khim. 10*, 1469−1482.

Welsh, K. M., Jacobyansky, A., Springs, B., & Cooperman, B. S. (1983) *Biochemistry 22*, 2243−2248.

BI962637U